Proceedings of PVP2008
2008 ASME Pressure Vessels and Piping Division Conference
July 21-31, 2008, Chicago, Illinois

PVP2008-61128

Treatment of High Temperature Tensile Data for Alloy 617 and Alloy 230*

T.-L. Sham — Oak Ridge National Laboratory, Oak Ridge, Tennessee, USA, Email: shamt@ornl.gov

D.R. Eno and K. P. Jensen — Lockheed Martin Corporation, Schenectady, New York, USA

ABSTRACT

Yield strength and tensile strength at temperature are used to set time independent primary stress limits for structural materials in various high temperature design codes. For the Ni-based Alloy 617 and HAYNES® 230® alloy[1] (Alloy 230), the temperature trends for the yield strength and tensile strength change significantly above around 1100*K* and 1025*K*, respectively, from the lower temperature trends. It is shown that standard methods in obtaining design values for these parameters for Very High Temperature Reactor applications are not satisfactory. Improved methods for the treatment of tensile data are proposed, resulting in more consistent and quantifiable design margin over the full range of low to high temperatures.

1.0 INTRODUCTION

Project Prometheus was initiated to develop a space nuclear/electric reactor system for a wide range of deep space and terrestrial missions. The basic concept was a compact fast reactor coupled with a direct gas Brayton cycle turbine that would drive on-board generators for electrical power, Fig 1. The Jupiter Icy Moon Orbiter (JIMO) mission was selected as the first mission and required operation for up to 15 years. This project was terminated in September of 2005 due to a shift in priorities at NASA. The following represents part of the efforts to support the development of preliminary structural design procedures for pre-conceptual structural component sizing analyses.

* This paper has been authored by a contractor of the U.S. Government under contract No. DE-AC12-00-SN39357. Accordingly, the U.S. Government retains a non-exclusive, royalty-free license to publish or reproduce the published form of this paper, or allows others to do so, for U.S. Government purposes.

[1] HAYNES and 230 are trademarks of Haynes International, Inc.

1.1 JIMO Pre-Conceptual Design

A number of preliminary designs of the JIMO pressure vessel and heat transport system were considered. One preliminary reactor design consisted of an outer vessel and an inner vessel, to be maintained at 900K and 1050K (max.) respectively. The hot gas leg was designed with a temperature of 1150K. Ni-based superalloys were being considered as the candidate materials for the reactor outer and inner vessels and the hot gas leg piping. Preliminary stress allowables for two Ni-base alloys were developed so that sizing analyses for this preliminary design could be performed to support trade studies. This paper considers the analysis of yield and tensile strengths to support the development of the time-independent stress limits.

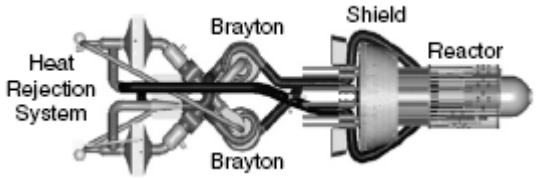

Fig. 1. Integrated layout of a pre-conceptual Prometheus reactor power system for the Jupiter Icy Moon Orbiter mission.

2.0 TENSILE DATA

Alloy 617 and Alloy 230 yield and tensile strength data from air tests were obtained from [1] and [2], respectively. The Alloy 617 database consists of 124 sets of yield and tensile strengths from 8 heats (annealed) and 4 product forms (bar, plate, sheet, and forging). There are 326 sets of yield and tensile strength data from 12 heats and 3 product forms (bar, plate, and sheet) for Alloy 230.

A plot of the yield and tensile strengths as a function of temperature is shown in Fig. 2 for Alloy 617 and Fig. 3 for Alloy 230. It is seen that the yield and tensile strengths decrease gradually as the temperature increases. However,

Copyright © 2008 by ASME

at temperatures beyond approximately 1000*K*, the temperature trends display much more rapid decays in strength than observed at lower temperatures.

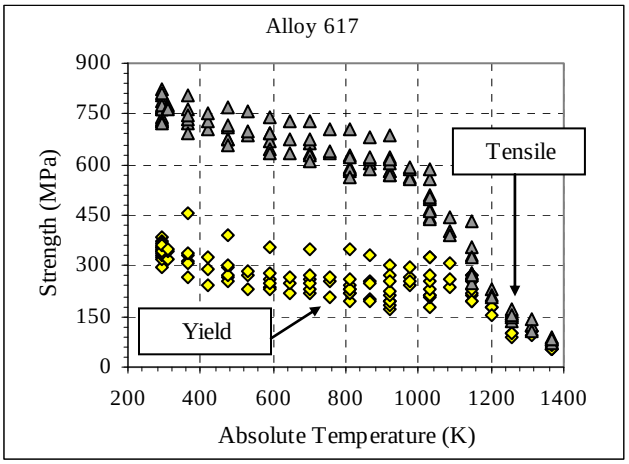

Fig. 2. Yield and tensile strengths for Alloy 617

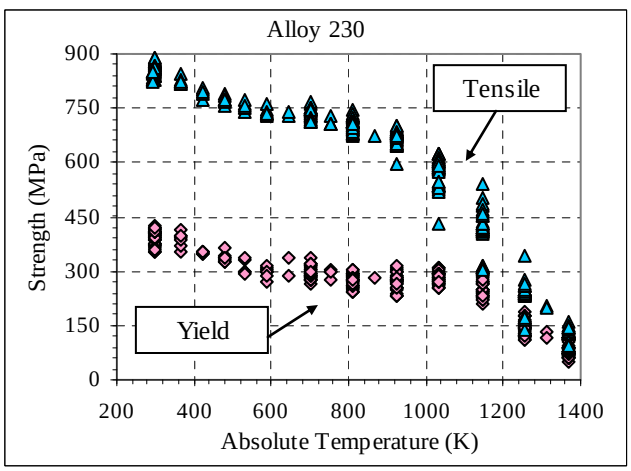

Fig. 3. Yield and tensile strengths for Alloy 230

It is also observed that while there is a wide separation of the yield and tensile strengths at lower temperatures, their scatter bands tend to converge and start to overlap at higher temperatures.

2.1 ASME Section II Procedures for Yield and Tensile Strengths

A procedure for developing the yield and tensile strengths at temperature for use in establishing the stress allowables is given in Appendix 2 of the ASME Boiler and Pressure Vessel Code, Section II, Part D. The yield strength at temperature is based on minimum values, and the tensile strength at temperature is based on average values. However, it is emphasized that "minimum" and "average" are not interpreted statistically in the ASME Code.

The steps involved in determining the minimum yield strength at temperature can be summarized as follows. The yield strength data for each heat are normalized by the room temperature yield strength for that heat, as a ratio of the yield strength at temperature to the room temperature strength. A best-fit trend curve, $R_Y(T)$, as a function of temperature, T, is then obtained by least square fit. It is customary that the trend curve is expressed in the form of a polynomial. The required minimum yield strength at temperature, $S_y(T)$, is defined as $S_Y R_Y(T)$ where S_Y is the specification minimum yield strength at room temperature.

The steps for determining the average tensile strength at temperature are similar to those for the minimum yield strength at temperature. The tensile strength data for each heat are normalized by the room temperature tensile strength for that heat, again as a ratio of tensile strength at temperature to room temperature strength. A best-fit trend curve, $R_T(T)$, is then obtained by least square fit. It is also customary that the tensile strength trend curve is expressed in the form of a polynomial. The required average tensile strength at temperature, $S_u(T)$, is set equal to $1.1 \times S_T R_T(T)$ where S_T is the specification minimum tensile strength at room temperature.

2.1.1 Alloy 617

The Section II procedures were followed to determine the minimum yield strength and average tensile strength at temperature for Alloy 617. Polynomials of third, fourth and fifth order were employed and it was determined that the third-order and fourth-order polynomials provide adequate fits to the normalized yield strength and tensile strength data, respectively. These fits are shown in Figs. 4 and 5. It is noted that due to the fluctuations inherent in polynomial

Copyright © 2008 by ASME

fits, extrapolations of these fits beyond the temperature ranges of the databases should not be considered stable.

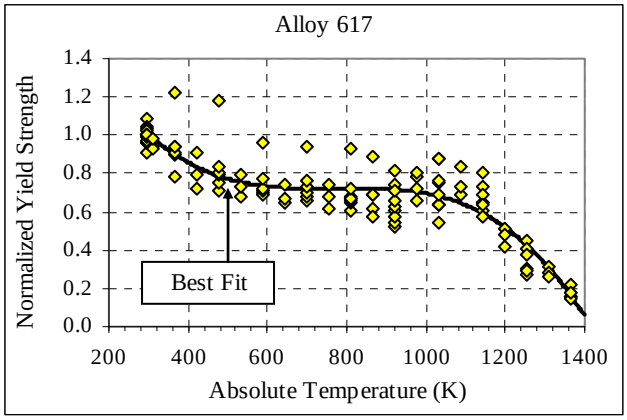

Fig. 4. Polynomial fit to normalized yield strength data

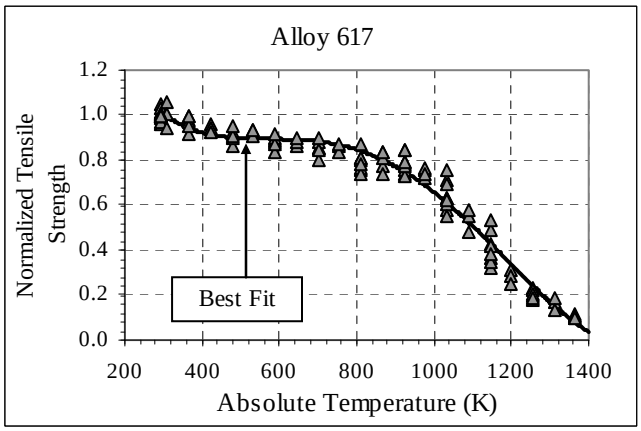

Fig. 5. Polynomial fit to normalized tensile strength data

Using the specification room temperature minimum yield strength of 240 MPa and minimum room temperature tensile strength of 655 MPa, [3], the minimum yield strength and average tensile strength curves for Alloy 617 were developed. They are shown in Fig. 6.

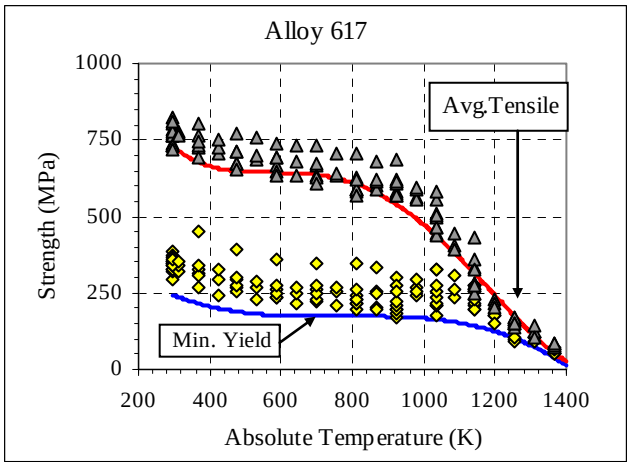

Fig. 6. Minimum yield strength and average tensile strength at temperature, Alloy 617

2.1.1 Alloy 230

Similarly, the Section II procedures were followed to determine the minimum yield strength and average tensile strength at temperature for Alloy 230. The best fits for the normalized yield and tensile strength data are shown in Figs. 7 and 8, respectively. Figure 9 shows the minimum yield and average tensile strength at temperature. The Alloy 230 specification room temperature minimum yield and tensile strengths of 310 MPa and 760 MPa [3], respectively, were used in developing the curves in Fig. 9.

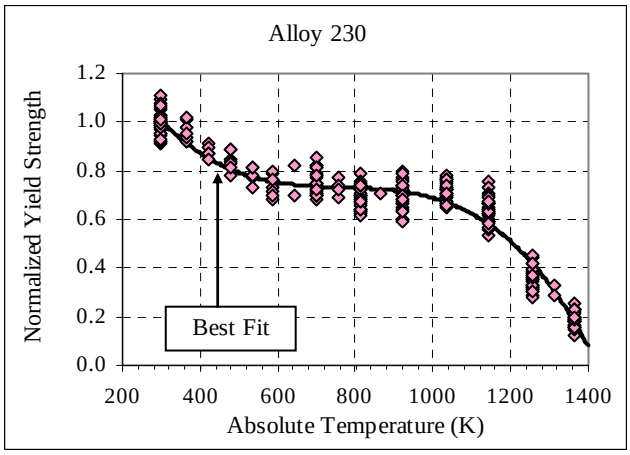

Fig. 7. Polynomial fit to normalized yield strength data

Copyright © 2008 by ASME

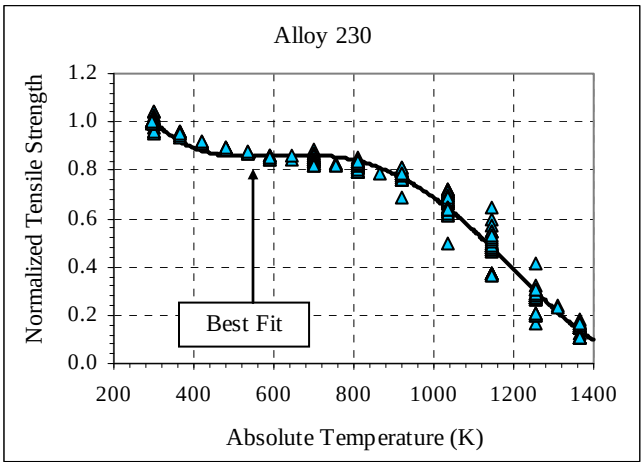

Fig. 8. Polynomial fit to normalized tensile strength data

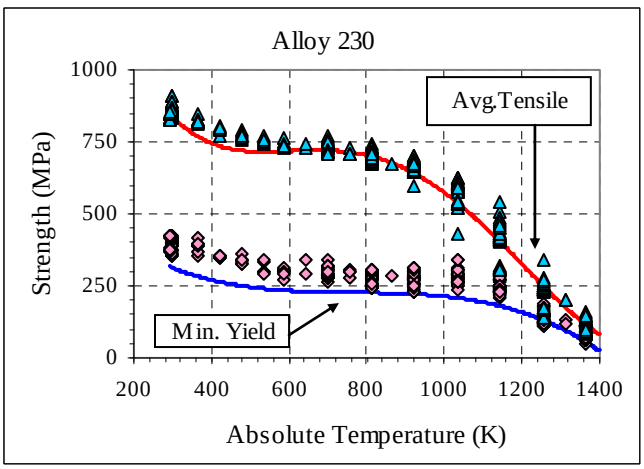

Fig. 9. Minimum yield strength and average tensile strength at temperature, Alloy 230

2.2 Analysis of the Section II Approach

The characteristics of the minimum yield strength and average tensile strength curves developed using the Section II methodology are analyzed in this section.

Let $\hat{S}_y(T)$ be the best-fit curve to the yield strength data. The vertical distance between the $\hat{S}_y(T)$ and $S_y(T)$ curves can be determined as

$$\begin{aligned}\hat{S}_y(T) - S_y(T) &= \hat{S}_y(T) - S_Y R_Y(T) \\ &\approx \hat{S}_y(T) - S_Y \frac{\hat{S}_y(T)}{\hat{S}_y(T_R)}\end{aligned} \qquad (1)$$

where T_R is room temperature (nominally 70 ºF). The approximation was made in equating $R_Y(T)$ to the ratio $\hat{S}_y(T)/\hat{S}_y(T_{Room})$. After re-arranging eqn. (1), the vertical distance between $\hat{S}_y(T)$ and $S_y(T)$ becomes

$$\hat{S}_y(T) - S_y(T) \approx c_y\ \hat{S}_y(T)\ ,\ c_y \equiv \left(1 - \frac{S_Y}{\hat{S}_y(T_{Room})}\right) \qquad (2)$$

The constant c_y is independent of temperature. Thus the vertical distance between $\hat{S}_y(T)$ and $S_y(T)$ is proportional to $\hat{S}_y(T)$, the best-fit yield strength curve. In the lower temperature range where $\hat{S}_y(T)$ does not decrease significantly with increasing temperature, the $S_y(T)$ curve lower-bounds the data adequately as the vertical distance between $\hat{S}_y(T)$ and $S_y(T)$ is not reduced appreciably.

But in the higher temperature range where the yield strength values drop off drastically, the best-fit and lower-bound curves approach each other as the vertical distance between the two curves is proportional to the best-fit yield strength, which decreases as the temperature increases. Since the data scatter in this higher temperature range is not smaller than that in the lower temperature range, the convergence of the $\hat{S}_y(T)$ and $S_y(T)$ curves undermines the ability of $S_y(T)$ to lower-bound the data in the high temperature regime.

Similar analysis shows that the vertical distance between the best-fit tensile strength curve, $\hat{S}_u(T)$, and the curve for the average tensile strength at temperature, $S_u(T)$, can be given approximately as

$$\hat{S}_u(T) - S_u(T) \approx c_u\ \hat{S}_u(T)\ ,\ c_u \equiv \left(1 - \frac{1.1 \times S_T}{\hat{S}_u(T_R)}\right) \qquad (3)$$

Again, the constant c_u is independent of temperature, and the vertical distance between $\hat{S}_u(T)$ and $S_u(T)$ is proportional to $\hat{S}_u(T)$, the best-fit tensile strength curve.

Copyright © 2008 by ASME

Thus the "margin" of the average tensile curve relative to the best-fit curve decreases as the temperature increases, particularly in the high temperature regime of interest.

In addition to the characteristics of the minimum and average strength curves discussed above, the use of "minimum" yield strength and "average" tensile strength to set the time-independent stress limits in the high temperature regime warrants further consideration. While this approach is satisfactory in the lower temperature range, as the tensile strengths are much higher than the yield strengths, such is not the case in the higher temperature regime. In fact, the scatter bands of yield and tensile strength data converge and start to overlap at high temperatures. Thus the use of minimum for one and average for the other is not consistent. It is noted that the "safety factor" on the yield strength is lower than that on the tensile strength, hence there is some form of compensating effect in setting the time-independent stress limits. However, such intermingling of data scatter and safety factor does not lend itself to a clear and consistent interpretation of overall margin.

An alternate approach is adopted to develop the yield strength and tensile strength curves for use in setting interim time-independent stress limits for Project Prometheus. This involves separating the consideration of data scatter from the judgment made on the design factors, and is achieved by characterizing the data scatter more precisely by using lower prediction bounds for both yield and tensile strength data. This approach thereby allows the selection of design factors on the yield and tensile strengths to be based only on the judgment of acceptable risk for the mission, separately from quantification of data scatter.

2.3 Lower Prediction Bounds

2.3.1 Yield strength

It is clear from Figs. 2 and 3 that the yield strength trend is not optimally modeled as a smooth function of temperature over the entire data range. A change in the temperature dependence of the yield strength is evident at about 1100*K* for Alloy 617 and 1125*K* for Alloy 230.

2.3.1.1 Alloy 617

In order to provide a better best-fit of the Alloy 617 yield strength data, exponential decay functions were chosen for the two temperature ranges:

$$S_y(T) = a_1 + b_1 \exp(c_1 T)\ , \quad \text{for } T < 1100K \tag{4}$$

$$S_y(T) = a_2 + b_2 \exp(c_2 T)\ , \quad \text{for } T \geq 1100K \tag{5}$$

where T is the absolute temperature in kelvin and a_1, b_1, c_1, a_2, b_2, and c_2 are estimated from the data. Parameter estimation was performed using least squares estimation over the entire temperature range, but with the regression parameters estimated independently over the low and high temperature ranges. Heat-to-heat variability was not explicitly accounted for in the analysis, as this was not considered critical for derivation of preliminary design curves. Such explicit accounting for heat-to-heat variability could be incorporated into the analysis if this were deemed necessary.

As a result of the independent estimation of regression parameters in the two temperature ranges, the intersection of the two exponential curves was left arbitrary. Following parameter estimation, this intersection was found to be at a temperature of 1137*K*. Since no data exist in the database between 1100*K* and 1137*K*, this intersection does not cause a re-definition of the low and high temperature groups. The fitted yield strength regression model for Alloy 617 is given by:

$$S_y(T) = 235.4 + 324.8 \exp(-0.003917T), \quad \text{for } T < 1137K \tag{6}$$

$$S_y(T) = -2.10 + 137829 \exp(-0.005581T), \quad \text{for } T \geq 1137K \tag{7}$$

Figures 10 and 11 display, respectively, measured versus predicted yield strength and a normal probability plot of the residuals from the fit of eqns. (6) and (7). Residual from the fitted regression model were examined for potential effects of product form on yield strength; no meaningful systematic variation was observed to suggest that the product forms should be treated separately.

Copyright © 2008 by ASME

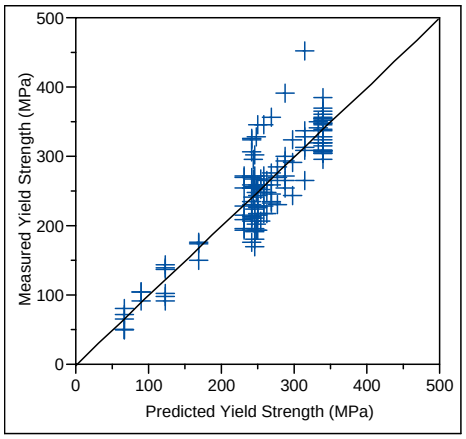

Fig. 10. Measured vs. predicted yield strength for Alloy 617

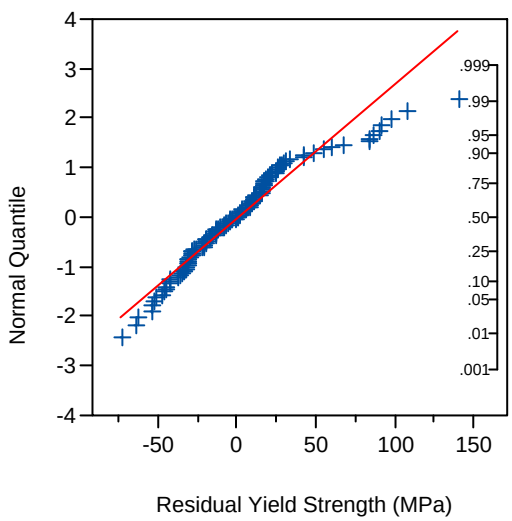

Fig. 11. Normal probability plot of residuals

For design purposes, a conservative lower bound for yield strength is required. The regression results can be used to define a lower prediction bound with an appropriate level of conservatism for use as a design curve. The intent of a prediction bound is to capture both the uncertainty in the mean yield strength and the individual measurement variability. The vertical distance between the best estimate and a prediction bound is dependent on temperature, with the distance minimized near the middle of the database and maximized at the temperature extremes of the database. Conceptually, this is due to the fact that predictions surrounded by supporting data are more reliable than predictions near the ends of the database, which have less locally supporting data. For simplicity of application, a constant "back-off" from best estimate is desired. The maximum predictive standard deviation over temperature less than 1200K, accounting for both model uncertainty and variability in the data, is 40.7 MPa. Therefore, conservative approximations to 100 P percent lower prediction bounds on Alloy 617 yield strength can be computed as

$$S_y(T) = 235.4 + 324.8\exp(-0.003917T) - 40.7z \quad \text{for } T < 1137K \tag{8}$$

$$S_y(T) = -2.10 + 137829\exp(-0.005581T) - 40.7z, \quad \text{for } 1137K \le T \le 1200K \tag{9}$$

where z denotes the 100 P^{th} percentile of the standard normal distribution. For P = 0.95, the value of z is 1.645. A plot of the best-fit curve and the 95% lower prediction bound (based on constant back-off) on Alloy 617 yield strength is shown in Fig. 12, together with the yield strength data.

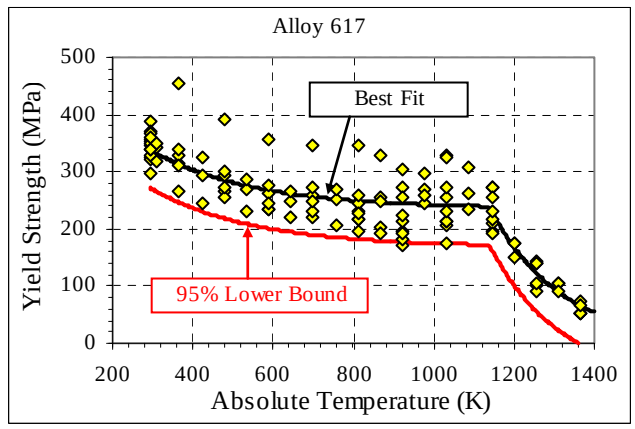

Fig. 12. Best fit and lower bound (constant back-off)

2.3.1.2 Alloy 230

Exponential decay models similar to eqns. (4) and (5) were used to fit the yield strength data over two temperature ranges for Alloy 230. However, based on the inspection of the data in Fig. 3, the break point for the low and high temperature behavior was chosen to be 1125K. The parameter estimation was performed using least squares estimation over the entire temperature range. The fitted yield strength regression model for Alloy 230 is given by

$$S_y(T) = 267.7 + 444.53\exp(-0.00411T) \quad \text{for } T < 1125K \tag{10}$$

$$S_y(T) = -21.84 + 56218\exp(-0.00467T) \quad \text{for } T \ge 1125K \tag{11}$$

Copyright © 2008 by ASME

Figures 13 and 14 display, respectively, measured versus predicted yield strength and a normal probability plot of the residuals from the fit of eqns. (10) and (11). Residuals from the fitted regression model were also examined for potential effects of product form on Alloy 230 yield strength; again, no meaningful systematic variation was observed to suggest that the product forms should be treated separately.

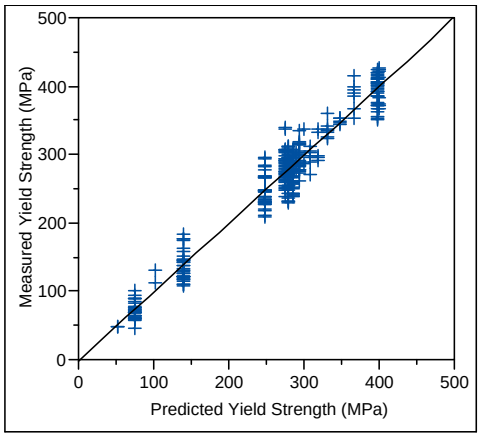

Fig. 13. Measured vs. predicted yield strength

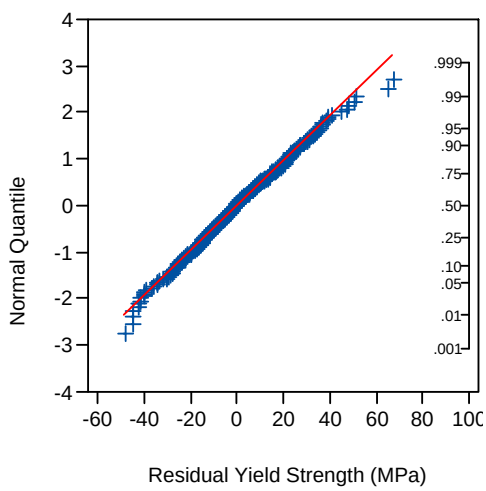

Fig. 14. Normal probability plot of residuals

As with Alloy 617, a lower prediction bound is desired for use as a design curve, and the vertical distance between the best estimate and the lower prediction bound is temperature dependent. For simplicity, a constant back-off from best estimate was adopted. The maximum predictive standard deviation over temperatures less than 1200*K*, accounting for both model uncertainty and variability in the data, is 21.0 MPa. Therefore, a conservative approximations to the 100 *P* percent lower prediction bound based on a constant back-off on Alloy 230 yield strength can be computed as

$$S_y(T) = 267.7 + 444.53\exp(-0.00411T) - 21.0z \quad \text{for } T < 1125K \tag{12}$$

$$S_y(T) = -21.84 + 56218\exp(-0.00467T) - 21.0z \quad \text{for } 1125K \le T \le 1200K \tag{13}$$

A plot of the best fit and the 95% lower prediction bound on Alloy 230 yield strength data is shown in Fig. 15, together with the yield strength data.

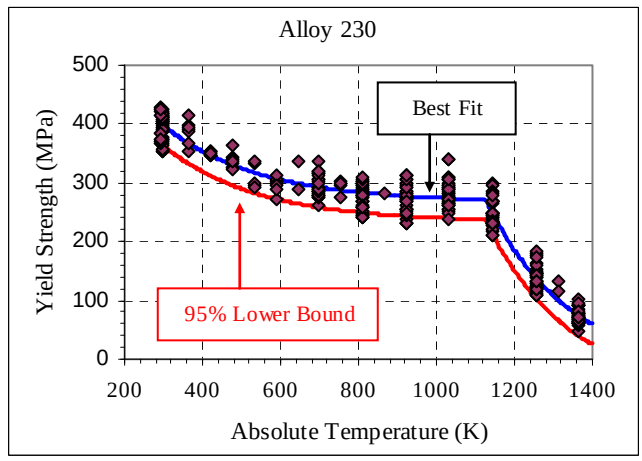

Fig. 15. Best fit and lower bound (constant back-off)

2.3.2 Tensile Strength

From Figs. 2 and 3, it is seen that the tensile strength drops gradually as the temperature increases. But at temperatures beyond 1000*K*, the decrease in the tensile strength is much more rapid.

2.3.2.1 Alloy 617

Exponential decay models were initially used to fit the tensile strength data over the low and high temperature ranges. However, over the low temperature range, the lack of curvature in the data led to instability of the coefficient estimates in the nonlinear regression model. Therefore, a linear model was used to fit the data over the low temperature range, and an exponential model was used over the high temperature range:

$$S_u(T) = a_1 + b_1 T\ , \quad \text{for } T < 1000K \tag{14}$$

$$S_u(T) = a_2 + b_2 \exp(c_2 T)\ , \quad \text{for } T \ge 1000K \tag{15}$$

Copyright © 2008 by ASME

where $T = 1000K$ was chosen as the break point. As a result of the independent estimation of regression parameters in the two temperature ranges, the intersection of the low temperature linear model and the high temperature exponential curve was left arbitrary. Following parameter estimation, this intersection was found to be at a temperature of $998K$. Since no data exist in the database between $998K$ and $1000K$, this intersection does not cause a re-definition of the low and high temperature groups. The fitted tensile strength regression model is given by

$$S_u(T) = 834 - 0.256T, \text{ for } T < 998K \tag{16}$$

$$S_u(T) = -131.7 + 19622\exp(-0.003325T) \quad \text{for } T \geq 998K \tag{17}$$

Figures 16 and 17 display, respectively, measured versus predicted tensile strength and a normal probability plot of the residuals from the fit of eqns. (16) and (17). Residuals from the fitted regression model were examined for potential effects of product form on the tensile strength; no meaningful systematic variation was observed to suggest that the product forms should be treated separately.

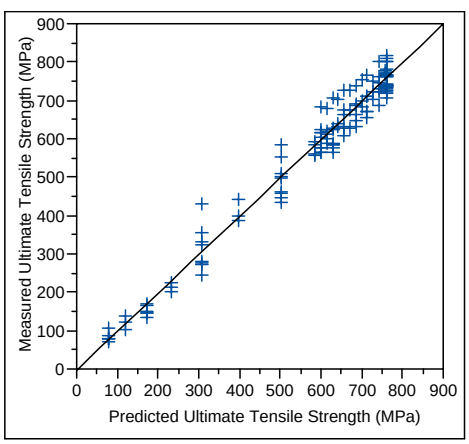

Fig. 16. Measured vs. predicted tensile strength

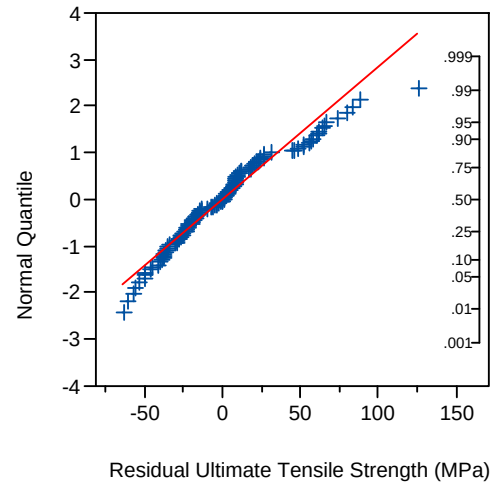

Fig. 17. Normal probability plot of residuals

The maximum predictive standard deviation over temperatures less than $1200K$, accounting for both model uncertainty and variability in the data, is 40.8 MPa. Therefore, a conservative approximation (based on a constant back-off) to a 100 P percent lower prediction bound on tensile strength can be computed as:

$$S_u(T) = 834 - 0.256T - 40.8z\,, \quad \text{for } T < 998K \tag{18}$$

$$S_u(T) = -131.7 + 19622\exp(-0.003325T) - 40.8z\,, \quad \text{for } 998K \leq T \leq 1200K \tag{19}$$

A plot of the best-fit curve and the 95% lower prediction bound on Alloy 617 tensile strength based on constant back-off are shown in Fig. 18, together with the tensile strength data.

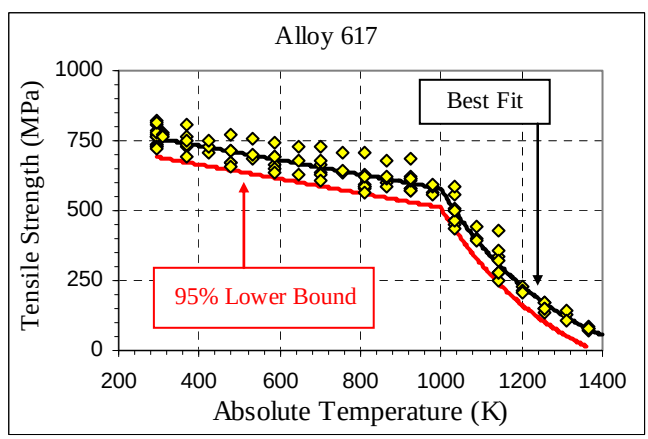

Fig. 18. Best fit and lower bound (constant back-off)

Copyright © 2008 by ASME

2.3.2.2 Alloy 230

The functional relationship between the tensile strength and temperature for Alloy 230 appears to be more complex than the relationship between the yield strength and temperature. The piecewise exponential model of eqns. (4) and (5) is not sufficiently flexible to capture the behavior exhibited by the tensile strength database. Instead, a three-part fit was found to provide a reasonable summary of the observed behavior. The following piecewise form, while purely empirical, is judged to be trustworthy for summary and interpolation:

$$S_u(T) = a_1 + b_1 \exp(c_1 T)\ , \quad \text{for } T \geq 775K \tag{20}$$

$$S_u(T) = a_2 + b_2 T + c_2 T^2\ , \quad \text{for } 775K \leq T < 1125K \tag{21}$$

$$S_u(T) = a_3 + b_3 \exp(c_3 T)\ , \quad \text{for } T \geq 1125K \tag{22}$$

Parameter estimation was performed using least squares estimation over the entire temperature range, with forced intersections at temperatures of 775*K* and 1125*K*. The fitted tensile strength regression model is given by

$$S_u(T) = 680.1 + 495.25 \exp(-0.00338T) \quad \text{for } T \geq 775K \tag{23}$$

$$S_u(T) = -589.9 + 3.359T - 0.00216T^2 \quad \text{for } 775K \leq T < 1125K \tag{24}$$

$$S_u(T) = -37.1 + 87090 \exp(-0.0046T) \quad \text{for } T \geq 1125K \tag{25}$$

Residuals from the fitted regression model were examined for potential effects of product form on tensile strength; no meaningful systematic variation was observed to suggest that the product forms should be treated separately.

Figure 19 displays the measured versus predicted tensile strength values; the model form of eqns. (23) to (25) appears to do an adequate job of summarizing the measured data. Figure 20 displays a normal probability plot of the residuals from the fit, and Fig. 21 displays the residuals versus temperature. It is evident from these two figures that the normal probability model is seriously deficient for summarizing the observed data scatter, and that the magnitude of data scatter is not constant over varying temperatures. Furthermore, it can be observed that at temperatures between 1000*K* and 1300*K*, low outliers are present relative to the bulk of the measured values. Therefore, even accounting for the heterogeneity of variance as a function of temperature would not allow for normal theory based prediction bands to be reliably interpretable with their nominal coverage levels.

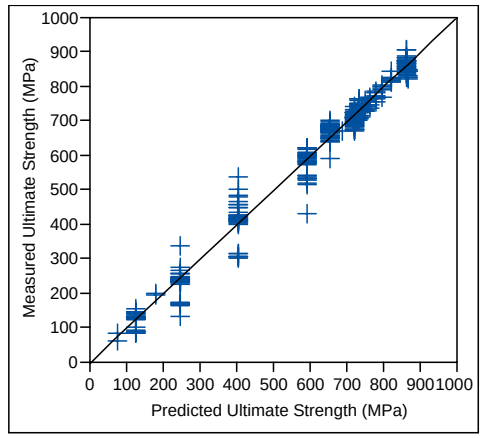

Fig. 19. Measured vs. predicted tensile strength

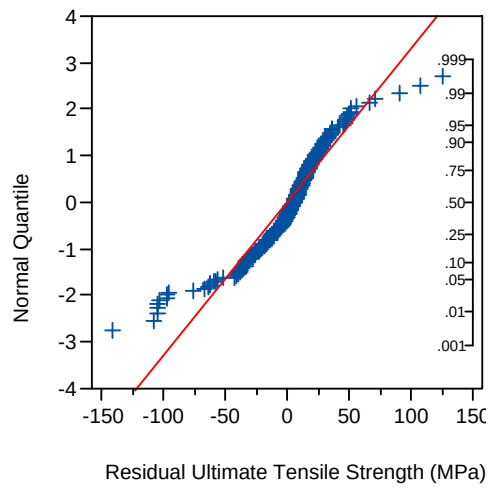

Fig. 20. Normal probability plot of residuals

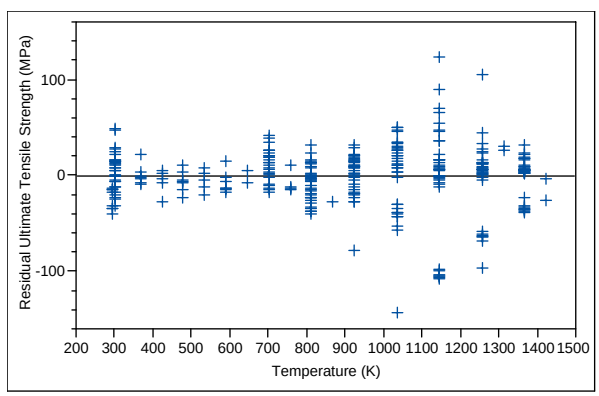

Fig. 21. Residual vs. temperature

Copyright © 2008 by ASME

To make an appropriate lower bound for tensile strength, the heterogeneity of variance was accounted for, and additional margin was added at the high temperature range to allow for reasonable coverage of the low outliers in the database. The resulting lower bound is displayed in Fig. 22, together with the best estimate of the tensile strength.

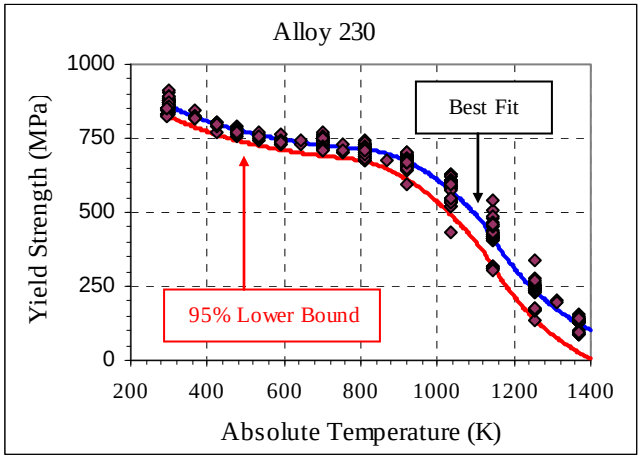

Fig. 22. Best fit and lower bound (constant back-off)

This bound is intended to provide approximately the same interpretation as a 95% lower prediction bound; however, due to the inability to fit an analytically tractable probability model to the data scatter, this interpretation is not backed by a strong theoretical basis. For use as preliminary design guidance for the JIMO pressure vessel and hot gas leg piping, this lower bound was nevertheless judged to be appropriate. This lower-bound is computed as

$$S_u(T) = 645.0 + 500.8\exp(-0.00342T) \quad \text{for } T \geq 775K \tag{26}$$

$$S_u(T) = -498.5 + 3.203T - 0.00217T^2 \quad \text{for } 775K \leq T < 1125K \tag{27}$$

$$S_u(T) = -135.7 + 83579\exp(-0.00456T) \quad \text{for } 1125K \leq T \leq 1200K \tag{28}$$

3.0 SUMMARY

Alloy 617 and Alloy 230 lower bound curves for the yield and tensile strengths at temperature were determined for JIMO reactor vessel and hot gas leg piping applications. This was done so that consideration of data scatter and selection of design factors on the yield and tensile strengths to set time-independent stress limits can be evaluated separately. This supports the development of adequately conservative preliminary design curves for sizing calculations in the pre-conceptual design of Prometheus reactor system for the JIMO mission. While this project was terminated in September of 2005 due to a shift in priorities at NASA, the results and methodologies presented herein could find applications in Very High Temperature Gas-Cooled Reactor concepts.

REFERENCES

[1] T.H. Bassford, Inconel 617 data package, Huntington Alloys, Inc., Huntington, WV, 1982
[2] M. Katcher, Haynes 230 data package, Haynes International, Inc., Kokomo, IN, 2004
[3] ASME Boiler and Pressure Vessel Code, Section II, Part B, ASME, New York, NY, 2007

Copyright © 2008 by ASME